Weak Ferromagnetism in Chiral 3-Dimensional Oxalato-Bridged Cobalt(II) Compounds. Crystal Structure of $[Co(bpy)_3][Co_2(ox)_3]ClO_4$

María Hernández-Molina,[†] Francesc Lloret,*[,‡] Catalina Ruiz-Pérez,*[,†] and Miguel Julve[‡]

Departament de Química Inorgànica, Facultat de Química de la Universitat de València, Dr. Moliner 50, 46100 Burjassot (València), Spain, and Grupo de Rayos X del Departamento de Física Fundamental y Experimental, Facultad de Física de la Universidad de la Laguna, Avda. Astrofísico Francisco Sánchez s/n, 38024 La Laguna (Tenerife), Spain

Received March 19, 1998

Introduction

The old but evergreen oxalate ligand has played a key role in the development of new concepts in molecular magnetism during the last two decades.[1−3] Its remarkable ability as a bis(chelating) ligand to mediate electronic effects between paramagnetic metal ions separated by more than 5.5 Å is at the origin of this.[4−7] Magneto−structural studies dealing with oxalato-bridged copper(II) dinuclear complexes have shown that the magnetic coupling can be tuned between zero and −386 cm^{-1} by playing on the denticity and number and nature of the substituents of the terminal amine ligand.[4−6] This antiferromagnetic coupling was gradually increased up to −800 cm^{-1} by substituting the oxalate oxygens by less electronegative atoms such as nitrogen and sulfur.[8−11] Theoretical studies were carried out on these systems in order to understand the structural and electronic factors that govern these trends.[12,13] More recently, subtle factors such as the influence of the nature of the peripheral donors atoms on the value of the magnetic coupling through oxalate and other bis(chelating) bridges were analyzed from both experimental and theoretical viewpoints.[14] The influence of the number of unpaired electrons on the magnetic coupling through oxalate was analyzed through the corresponding magneto−structural investigations concerning oxalato-bridged dinuclear species with first-row transition metal ions other than copper(II).[15,16] Finally, basic knowledge on the first ferrimagnetic bimetallic chains and examples of high-spin molecules were provided by heterometallic oxalato-containing compounds.[17,18]

Recently, the oxalate ion has allowed the construction of two-[19−27] and three-dimensional[28−30] transition metal networks which have appplications as molecular-based magnetic materials. The synthetic strategy consists of polymerizing the $[M(ox)_3]^{(6-m)-}$ chiral mononuclear precursor into two or three directions. The honeycomb layered structure (2D) results when the precursors of different chirality are alternatively linked, whereas the 3D arises by assembling building blocks of the same chirality. The formation of the 2D or 3D framework structure is dependent on the choice of the templating counterion. So, 2D honeycomb layer structures of formula $[M^{II}M^{III}(ox)_3]^-$ (M^{II} = V, Cr, Mn, Fe, Co, Ni, Cu, Zn; M^{III} = V, Cr, Fe) were obtained with $[XR_4]^+$ cations (X = N, P; R = phenyl, *n*-propyl, *n*-butyl, *n*-pentyl). However, the use of the tris-chelated transition-metal diimine complexes $[M(bpy)_3]^{m+}$ (bpy = 2,2′-bipyridine; m = 2, 3) led to chiral 3D networks of formula $[M^{II}_2(ox)_3]^{2-}$, $[M^IM^{III}(ox)_3]^{2-}$, and $[M^{II}M^{III}(ox)_3]^-$ where the cation and anion are enantiomers. These polymeric 2D and 3D materials exhibit a great diversity of magnetic behaviors, ferro-, ferri-, or antiferromagnetic long-range ordering being observed. Single-crystal field-dependent magnetization measurements coupled with elastic neutron diffraction experiments were carried out on the 2D compound $\{[P(C_6D_5)_4](Mn^{II}Cr^{III}(ox)_3]\}$ to fully characterize the ferromagnetic ordering that it exhibits at temperatures below $T_c = 6$ K.[27]

In this work, we present the preparation, crystal structure determination, and magnetic characterization of the compound

---

* To whom correspondence should be addressed.

[†] Grupo de Rayos X, Departamento de Física Fundamental y Experimental, Universidad de la Laguna.

[‡] Departament de Química Inorgànica, Universitat de València.

(1) Kahn, O. *Angew. Chem., Int. Ed. Engl.* **1985**, *24*, 834.

(2) Kahn, O. *Molecular Magnetism*; VCH: Weinheim, Germany, 1993.

(3) Decurtins, S.; Schmalle, H. W.; Pelleaux, R.; Fischer, P.; Hauser, A. *Mol. Cryst. Liq. Cryst.* **1997**, *305*, 227.

(4) Felthouse, T. R.; Laskowski, E. J.; Hendrickson, D. N. *Inorg. Chem.* **1977**, *16*, 6, 1077.

(5) Julve, M.; Verdaguer, M.; Gleizes, A.; Philoche-Levisalles, M.; Kahn, O. *Inorg. Chem.* **1984**, *23*, 3808.

(6) (a) Julve, M.; Faus, J.; Verdaguer, M.; Gleizes, A. *J. Am. Chem. Soc.* **1984**, *106*, 6, 8306. (b) Gleizes, A.; Julve, M.; Verdaguer, M.; Real, J. A.; Faus, J.; Solans, X. *J. Chem. Soc., Dalton Trans.* **1992**, 3209.

(7) Soto, L.; García, J.; Escrivá, E.; Legros, J. P.; Tuchagues, J. P.; Dahan, F.; Fuertes, A. *Inorg. Chem.* **1989**, *28*, 3378.

(8) Verdaguer, M.; Kahn, O.; Julve, M.; Gleizes, A. *Nouv. J. Chim.* **1985**, *9*, 325.

(9) (a) Veit, R.; Girerd, J. J.; Kahn, O.; Robert, F.; Jeannin, Y. *Inorg. Chem.* **1986**, *25*, 4175 and references therein. (b) Journaux, Y.; Lloret, F.; Kahn, O. *Inorg. Chem.* **1990**, *29*, 3048.

(10) Vicente, R.; Ribas, J.; Alvarez, S.; Seguí, A.; Solans, X.; Verdaguer, M. *Inorg. Chem.* **1987**, *26*, 4004.

(11) Okawa, H.; Matsumoto, N.; Koikawa, M.; Takeda, K.; Kida, S. *J. Chem. Soc., Dalton Trans.* **1990**, 1383.

(12) Charlot, M. F.; Verdaguer, M.; Journaux, Y.; De Loth, P.; Daudey, J. P. *Inorg. Chem.* **1984**, *23*, 3802.

(13) Alvarez, S.; Julve, M.; Verdaguer, M. *Inorg. Chem.* **1990**, *29*, 4500.

(14) Roman, P.; Guzmán-Miralles, C.; Luque, A.; Beitia, J. I.; Cano, J.; Lloret, F.; Julve, M.; Alvarez, S. *Inorg. Chem.* **1996**, *35*, 3741.

(15) Ohba, M.; Tamaki, H.; Matsumoto, N.; Okawa, H. *Inorg. Chem.* **1993**, *32*, 5385.

(16) Glerup, J.; Goodson, P. A.; Hodgson, D. J.; Michelsen, K. *Inorg. Chem.* **1995**, *34*, 6255.

(17) Verdaguer, M.; Julve, M.; Michalowicz, A.; Kahn, O. *Inorg. Chem.* **1983**, *22*, 2, 2624.

(18) Pei, Y.; Journaux, Y.; Kahn, O. *Inorg. Chem.* **1989**, *28*, 100.

(19) Tamaki, H.; Zhong, Z. J.; Matsumoto, N.; Kida, S.; Koikawa, M.; Achiwa, N.; Hashimoto, Y.; Okawa, H. *J. Am. Chem. Soc.* **1992**, *114*, 6974.

(20) Atovmyan, L. O.; Shilov, G. V.; Lyubovskaya, R. N.; Zhilyaeva, E. I.; Ovanesyan, N. S.; Pirumova, S. I.; Gusakovskaya, I. G. *JETP Lett.* **1993**, *58*, 766.

(21) Decurtins, S.; Schmalle, H. W.; Oswald, H. R.; Linden, A.; Ensling, J.; Gütlich, P.; Hauser, A. *Inorg. Chim. Acta* **1994**, *216*, 65.

(22) Reiff, W. M.; Kreisz; Meda, L.; Kirss, R. U. *Mol. Cryst. Liq. Cryst.* **1995**, *273*, 181.

(23) Farrell, R. P.; Hambley, T. W.; Lay, P. A. *Inorg. Chem.* **1995**, *34*, 757.

(24) Mathonière, C.; Nuttall, C. J.; Carling, S. G.; Day, P. *Inorg. Chem.* **1996**, *35*, 5, 1201.

(25) Carling, S. G.; Mathonière, C.; Day, P.; Malik, K. M. A.; Coles, S. J.; Hursthouse, M. B. *J. Chem. Soc., Dalton Trans.* **1996**, 1839.

(26) Bhattacharjee, A.; Iijima, S.; Mitzutani, F. *J. Magn. Magn. Mater.* **1996**, *235*, 153.

(27) Pellaux, R.; Schmalle, H. W.; Huber, R.; Fischer, P.; Hauss, T.; Ouladdiaf, B.; Decurtins, S. *Inorg. Chem.* **1997**, *36*, 2301.

(28) Decurtins, S.; Schmalle, H. W.; Schneuwly, P.; Oswald, H. R. *Inorg. Chem.* **1993**, *32*, 1888.

(29) (a) Decurtins, S.; Schmalle, H. W.; Schneuwly, P.; Ensling, J.; Gütlich, P. *J. Am. Chem. Soc.* **1994**, *116*, 9521. (b) Decurtins, S.; Schmalle, H. W.; Pellaux, R.; Huber, R.; Fisher, P.; Ouladdiaf, B. *Adv. Mater.* **1998**, *8*, 647.

(30) Decurtins, S.; Schmalle, H. W.; Pellaux, R.; Schneuwly, P.; Hauser, A. *Inorg. Chem.* **1996**, *35*, 1451.

(31) Burstall, F. H.; Nynolm, R. S. *J. Chem. Soc.* **1952**, 3570.

S0020-1669(98)00306-1 CCC: $15.00

of formula $[Co^{III}(bpy)_3][Co^{II}_2(ox)_3]ClO_4$ (**1**) where two different counterions ($[Co(bpy)_3]^{3+}$ and ClO_4^-) induce the crystallization of the chiral 3D $[Co_2(ox)_3]^{2-}$ anionic network. The magnetic properties of the isostructural $[M^{II}(bpy)_3][Co^{II}_2(ox)_3]$ [M^{II} = Fe (**2**) and Ni (**3**)] compounds are also reported for comparative purposes.

Experimental Section

Materials. All chemicals were of reagent grade and were used as commercially obtained. Standard literature procedures were used to prepare the starting tris-chelated compounds $[Co(bpy)_3]Cl_3$, $[Fe(bpy)_3]Cl_2$, and $[Ni(bpy)_3]Cl_2$.[31,32] Elemental analyses (C, H, N) were performed on an Eager 200 1108 CHNS-0 microanalytical analyzer. Metal contents were determined by absorption spectrometry.

Preparation of $[Co^{III}(bpy)_3][Co^{II}_2(ox)_3]ClO_4$ (1). To a 0.01 M aqueous solution of the $[Co(bpy)_3]Cl_3$ salt, a stoichiometric quantity of the $[Co(H_2O)_6](ClO_4)_2$ salt was added with stirring at room temperature. To the clear solution, a stoichiometric quantity of 0.02 M aqueous oxalic acid was added slowly, and **1** separates as a red microcrystalline precipitate on standing. It was filtered off, washed with warm water, ethanol, and diethyl ether, and dried in air. Anal. Calcd for $C_{36}H_{24}ClCo_3N_6O_{16}$ (**1**): C, 42.86; H, 2.40; N, 8.33; Co, 17.53. Found: C, 42.48; H, 2.38; N, 8.49; Co, 17.25%. [**Caution!** *Perchlorate salts of metal complexes can be explosive and must be handled with care. We only prepare and use small amounts (mmol scale) of these kinds of complexes in our current work*].

Single crystals of **1** as red cubes were prepared by slow diffusion techniques in a H-shaped tube containing aqueous solutions of oxalic acid in one arm and a mixture of $[Co(bpy)_3]Cl_3$ and $[Co(H_2O)_6](ClO_4)_2$ salts in the other arm.

Preparation of $[M^{II}(bpy)_3][Co^{II}_2(ox)_3]$ [M^{II} = Fe (2) and Ni (3)]. These compounds were synthesized by a previously reported method.[29a] Their X-ray powder diffraction data showed them to be isostructural with **1**.

Magnetic Measurements. Magnetic susceptibility, magnetization, and ac measurements were performed on polycrystalline samples of compounds **1**−**3** with a Quantum Design SQUID susceptometer covering the temperature range 2.0−300 K and using applied magnetic fields ranging from a few gauss to 5 T. Amplitudes of 1 G and different frequencies were used to carry out the ac measurements. The susceptometer was calibrated with $(NH_4)_2Mn(SO_4)_2\cdot 12H_2O$. The experimental susceptibilty data were corrected for the diamagnetism estimated from Pascal's tables [-456×10^{-6} (**1**), -427×10^{-6} (**2**), and -426×10^{-6} cm^3 mol^{-1} (**3**)], and the temperature-independent paramagnetism (TIP) was taken to be 200×10^{-6} cm^3 mol^{-1} for **1**−**3**.[33]

X-ray Crystallographic Analysis. A quasi cubic crystal of **1** of approximate dimensions 0.37 × 0.33 × 0.32 mm was mounted on a Siemens AED automatic four-circle diffractometer and used for data collection. Diffraction data were collected at 293 K with graphite-monochromated Cu Kα radiation (λ = 1.541 79 Å) and using the $\omega-2\theta$ scan technique. Relevant crystallographic data and structure determination parameters for complex **1** are given in Table 1. Unit cell parameters and orientation matrix were determined by least-squares treatment of the setting angles of 20 reflections in the $5 < \theta < 15°$ range.[34] Examination of two standard reflections, monitored every 2 h, showed no sign of crystal deterioration. The index ranges of data collection were $0 \le h \le 17$, $-16 \le k \le 16$, and $-11 \le l \le 12$. Intensity data were corrected for Lorentz−polarization and absorption.[35] The maximum and minimum transmission factors were 0.145 and 0.065.

The structure of **1** was solved by direct methods followed by successive Fourier syntheses through SIR92.[36] Non-hydrogen atoms were refined anisotropically by full-matrix least-squares techniques on F^2 by using the SHELXL-93[37] computational program. Of the 869 measured independent reflections in the θ range 4.09−59.18°, 511 having $I \ge 2\sigma(I)$ were considered as observed and used in the analysis. The hydrogen atoms of bpy were set in calculated positions and refined as riding atoms. The O(3) and O(4) perchlorate oxygen atoms are in special positions, and they are affected with a considerable disorder degree as shown by their high anisotropy and thermal displacement parameters. A better localization of these atoms could not be obtained. The final Fourier-difference map showed maximum and minimum height peaks of 0.26 and −0.38 e Å^{-3}, respectively. The largest and mean Δ/σ are −0.009 and 0.002. The goodness-of-fit is 0.898. The final geometrical calculations and the graphical manipulations were carried out with the PARST95[38] and ORTEPII[39] programs, respectively. Main interatomic bond distances and angles are listed in Table 2.

Table 1. Crystallographic Data for $[Co^{III}(bpy)_3][Co^{II}_2(ox)_3]ClO_4$ (**1**)

formula	$C_{36}H_{24}ClCo_3N_6O_{16}$
fw	1008.85
space group	$P4_132$
a, Å	15.287(2)
V, Å^3	3572.5(8)
Z	8
T, K	293
ρ_{calcd}, g cm^{-3}	1.876
λ, Å	1.541 79
μ(Cu Kα), mm^{-1}	12.27
R^a	0.0523
$R_w{}^{b,c}$	0.0958

[a] $R = \sum||F_o| - |F_c||/\sum|F_o|$. [b] $R_w = [\sum w(F_o^2 - F_c^2)^2/\sum(F_o^2)^2]^{1/2}$. [c] $w = 1/\sigma^2(F_o)^2 + 0.0526P)^2 + 0.000P]$, where $P = (F_o^2 + 2F_o^2)/3$.

Results and Discussion

Description of the Structure of 1. The structure of **1** is made of the anionic 3D network $[Co_2(ox)_3]^{2-}$ with uncoordinated perchlorate and tris-chelated cobalt(III) cations $[Co(bpy)_3]^{3+}$ occupying its vacancies. A perspective view of the tris(oxalato)cobaltate(II) unit with the atomic numbering is shown in Figure 1. The oxalate ligands repeatedly bridge adjacent Co(2) atoms in all three dimensions leading to a polymeric net. It can be seen how the Λ-configuration of the chiral $[Co(ox)_{3/2}]$ subunits produces right-handed helical strands. [100] projections showing the anionic host ($[Co_2(ox)_3]^{2-}$) and the two guests ($[Co(bpy)_3]^{3+}$ and ClO_4^-) are depicted in Figure 2a,b. The tris-chelating $[Co(bpy)_3]^{3+}$ ions are found to be in the Λ-configuration. Electrostatic interactions as well as weak C−H(bpy)···O(oxalate) hydrogen bonds (see end of Table 2) ensure the cohesion of the crystal lattice. The size of the holes of the anionic framework (average diameter of 9.043 Å) is large enough to encapsulate the two guests. The accumulation of positive charge from the tripositive cations accounts for the encapsulation of the anionic perchlorate. It is located at the center of the cavity built by three hosted tripositive cations, the site symmetry for the hosted species having a crystallographically imposed symmetry in the form of a 3-fold axis (see Figure 3). These structural features were recently reported for the isostructural compounds of formula $[Cr(bpy)_3][Mn_2(ox)_3]ClO_4$ and $[Cr(bpy)_3][Mn_2(ox)_3]BF_4$.[30]

The cobalt(II) ions are octahedrally surrounded by three bis(chelating) oxalato in a quasi D_3 symmetry. The Co−O bond

---

(32) Palmer, R. A.; Piper, T. S. *Inorg. Chem.* **1966**, *5*, 864.

(33) Casey, T. In *Theory and Application of Molecular Paramagnetism*; Boudreaux, E. A., Mulay, L. N., Eds.; John Wiley & Sons: New York, 1976; Chapter 2.

(34) *Stoe & Cie. RE004 Data Reduction Program*, version 6.2D; Stoe & Cie: Darmstadt, Germany, 1992.

(35) González-Platas, J.; Ruiz-Pérez, C. *NEWCORR Program for empirical absorption correction*; University of La Laguna: La Laguna, Spain, 1997.

(36) Altomare, A.; Cascarano, G.; Giacovazzo, C.; Guagliardi, A.; Burla, M. C.; Polidori, G.; Camalli, M. SIR92 program for the resolution of structures by direct methods, 1994.

(37) Sheldrick, G. M. *SHELX93*: *Program for Crystal Structure Refinement*; University of Göttingen: Göttingen, Germany, 1993.

(38) Nardelli, M. PARST95. *J. Appl. Crystallogr.* **1995**, *28*, 659.

(39) Brueggemann, R.; Schmidt, G. PC adaptation of ORTEP, University of Ulm, Germany, 1990.

Table 2. Selected Bond Lengths (Å) and Angles (deg)[a,b] for Compound **1**

Metal			
Co(III) environment		Co(II) environment	
Co(1)−N(1)	1.914(5)	Co(2)−O(1)	2.081(5)
		Co(2)−O(2)	2.070(5)
N(1)$^{\mathrm{i}}$−Co(1)−N(1)	93.6(2)	O(2)$^{\mathrm{ii}}$−Co(2)−O(2)	90.8(2)
N(1)$^{\mathrm{ii}}$−Co(1)−N(1)	175.3(4)	O(2)$^{\mathrm{ii}}$−Co(2)−O(1)	171.4(2)
N(1)$^{\mathrm{iii}}$−Co(1)−N(1)	89.9(4)	O(2)$^{\mathrm{v}}$−Co(2)−O(1)	91.7(2)
N(1)$^{\mathrm{iv}}$−Co(1)−N(1)	83.1(4)	O(2)−Co(2)−O(1)	81.0(2)
		O(1)−Co(2)−O(1)$^{\mathrm{ii}}$	96.7(2)
		C(6)−O(1)−Co(2)	113.2(5)
		C(7)−O(2)−Co(2)	113.9(5)
Oxalate Ligand			
C(6)−C(7)	1.590(2)	C(6)−O(1)	1.271(6)
		C(7)−O(2)	1.271(7)
O(1)$^{\mathrm{iv}}$−C(6)−O(1)	128.2(10)	O(2)$^{\mathrm{iv}}$−C87)−O(2)	128.9(10)
O(1)$^{\mathrm{iv}}$−C(6)−C(7)	115.9(5)	O(2)$^{\mathrm{iv}}$−C(7)−C(6)	115.5(5)
O(1)−C(6)−C(7)	115.9(5)	O(2)−C(7)−C(6)	115.5(5)
2,2′-Bipyridine Ligand			
N(1)−C(1)	1.347(9)	C(1)−C(2)	1.398(10)
N(1)−C(5)	1.369(9)	C(2)−C(3)	1.373(12)
		C(3)−C(4)	1.359(10)
		C(4)−C(5)	1.416(11)
		C(5)−C(5)$^{\mathrm{iv}}$	1.423(14)
C(1)−N(1)−C(5)	118.4(6)	C(3)−C(4)−C(5)	119.5(8)
N(1)−C(1)−C(2)	122.4(8)	N(1)−C(5)−C(4)	120.6(6)
C(3)−C(2)−C(1)	118.7(89	N(1)−C(5)−C(5)$^{\mathrm{v}}$	114.1(4)
C(4)−C(3)−C(2)	120.1(8)	C(4)−C(5)−C(5)$^{\mathrm{v}}$	125.3(4)

Hydrogen-Bonding Contacts[c]

A	D	H	H···A, Å	A···D, Å	A···D−H, deg
O(1)$^{\mathrm{vi}}$	C(1)	H(1)	2.629(10)	3.201(10)	120.3(8)
O(2)$^{\mathrm{iv}}$	C(4)	H(4)	2.520(9)	3.390(9)	155.75(8)

[a] Estimated standard deviations in the last significant digits are given in parentheses. [b] Symmetry code: (i) $-x + {}^{1}/_{2}, -y + 1, z + {}^{1}/_{2}$; (ii) $-x + {}^{3}/_{4}, -y + {}^{3}/_{4}, -z + {}^{3}/_{4}$; (iii) $x - {}^{1}/_{4}, -y + {}^{5}/_{4}, z + {}^{1}/_{4}$; (iv) $x + {}^{1}/_{4}, y - {}^{1}/_{4}, -z + {}^{1}/_{4}$; (v) x, y, z; (vi) $x + {}^{1}/_{4}, y + {}^{3}/_{4}, -z + {}^{1}/_{4}$.

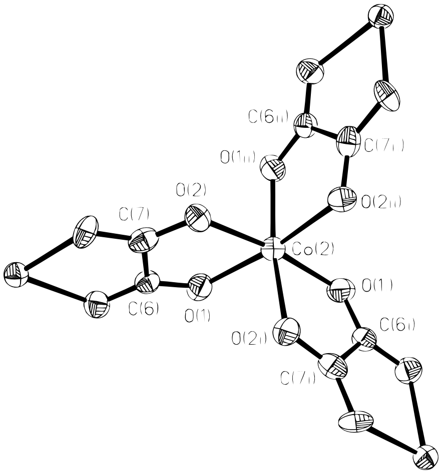

Figure 1. ORTEP drawing of the Co(2) coordination in the three-dimensional Co(II)−oxalato network of compound **1**. Thermal ellipsoids are drawn at the 50% probability level.

lengths of 2.081(5) and 2.070(5) Å are very close to that reported for the oxalato-bridged dinuclear cobalt(II) complex of formula [Co_2(bipicen)$_2$(ox)](ClO_4)$_2$·H_2O (bispicen = *N*,*N*′-bis(2-pyridylmethyl)-1,2-ethanediamine) [average value 2.094(2) Å],[40] and

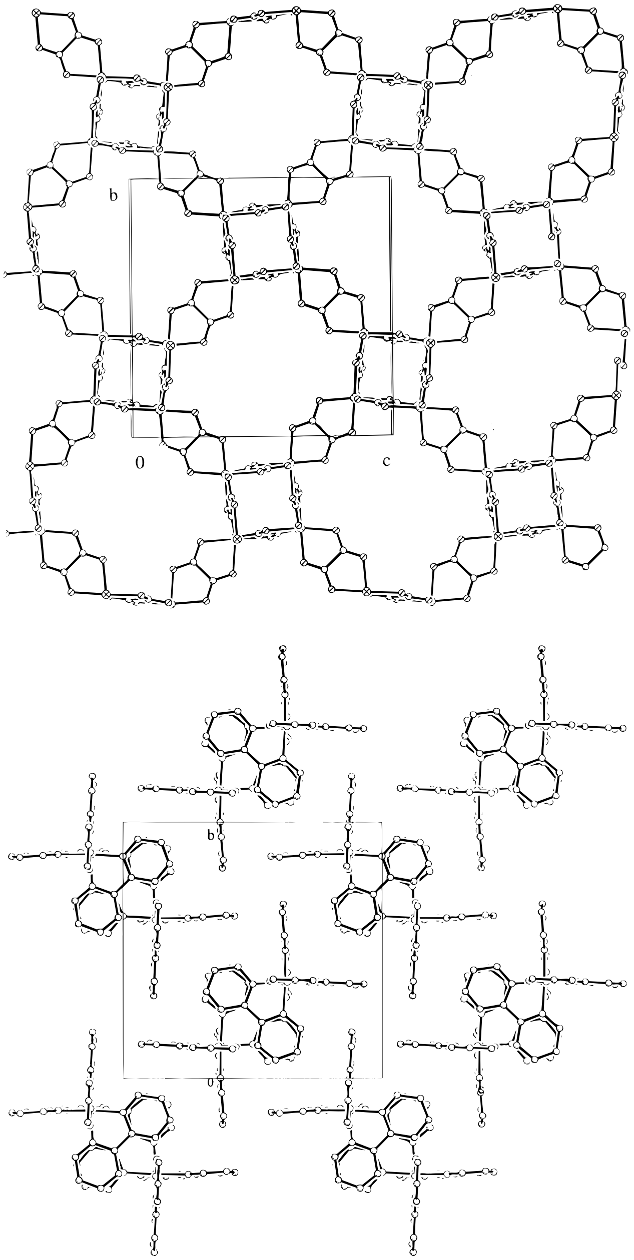

Figure 2. [100] projection of (a, top) $[Co_2(ox)_3]^{2-}$ and (b, bottom) $[Co(bpy)_3]^{3+}$ for compound **1**.

they are longer than that observed in the tris(oxalato)cobaltate(III) anion (mean Co−O distances ranging from 1.925 to 1.897 Å), as expected due to the higher oxidation state of the cobalt atom in the latter.[41] The angle subtended at the cobalt atom by the oxalate ligand is 81.0(2)°. An adequate description of the trigonally distorted octahedral CoO_6 unit is given by means of two structural parameters, namely the degree of compression (*s*/*h*) and the angle of twisting (ϕ).[42] The values for these parameters in the case of a perfect octahedron are 1.22 and 60°, respectively. The tris(oxalato)cobalt complex reveals an *s*/*h* ratio of 1.36 [$s = 3.029$ Å (mean value), $h = 2.229$ Å] and an angle ϕ of 50.9°. The oxalate ligand is quite planar [largest deviation is 0.024(5) Å at O(2)], and the Co(2) atom is 0.156(2) Å out of this mean plane. The values of the dihedral angle between the oxalate mean planes vary in the range 91.7(3)−

---

(40) Glerup, J.; Goodson, P. A.; Hodgson, D. J.; Michelsen, K. *Inorg. Chem.* **1995**, *34*, 6255.

(41) Butler, K. R.; Snow, M. R. *J. Chem. Soc. A* **1971**, 565. Okazaki, H.; Kushi, Y.; Yoneda, H. *J. Am. Chem. Soc.* **1985**, *107*, 4183.

(42) Stiefel, E. I.; Brown, G. F. *Inorg. Chem.* **1972**, *11*, 434.

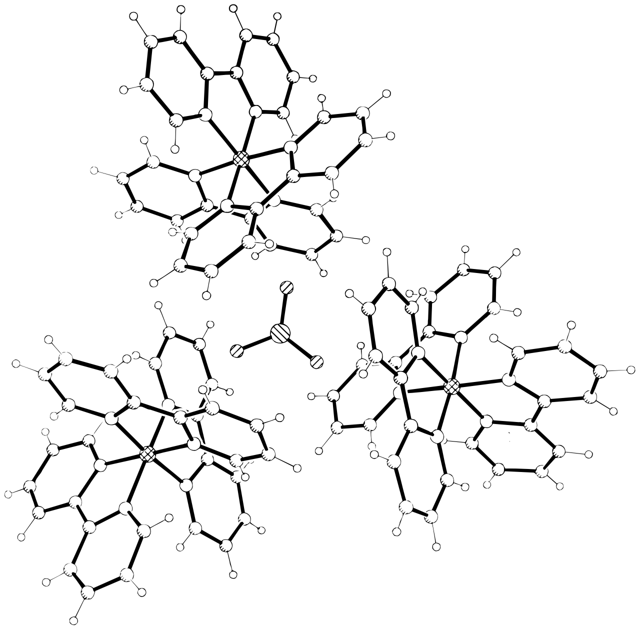

Figure 3. Perspective view showing the location of the perchlorate anion among the tris-chelated cobalt(III) cations.

87.9(4)°. The C−O bond lengths in the oxalate ligand are equal (1.271(6) and 1.271(7) Å), and they are normal for bis(chelating) coordination. The C−C bond of 1.590(2) Å is significantly longer than the values of 1.50−1.54 Å, usually observed in coordinated oxalate. It is even slightly longer than that observed in uncoordinated oxalate (1.574(2) Å).[43] The metal−metal separation across the oxalato bridge is 5.440(2) Å.

The six coordinated nitrogen atoms of three bpy ligands form a distorted octahedron around the cobalt(III) ion. As in the preceding tris(oxalato)cobaltate(II) unit, the $[Co(bpy)_3]^{3+}$ entity exhibits a quasi D_3 symmetry. The values of the ratio s/h and the angle ϕ are 1.35 and 54.45°, respectively. The values of the Co(1)−N(1) bond length and that of the angle subtended at the cobalt atom by the bpy ligand are 1.914(5) Å and 83.1(4)°, respectively. They compare well with the mean Co−N (1.932 Å) and N−Co−N (83.2°) values observed in the compound $(-)_D$-$[Co(bpy)_3][Fe(CN)_6]\cdot 8H_2O$.[44] A significant lengthening of the Co−N bond distance (average value 2.128(8) Å) and a shortening of the N−Co−N bite angle (mean value 76.5(8)°) were observed in the tris-chelating $Co(bpy)_3]^{2+}$ unit because of the lower oxidation state of the cobalt atom in this species.[45] The average C−C and C−N bond lengths within the bpy groups are 1.386(13) (1.423(14) Å for C(5)−C(5)^{iv}) and 1.358(9) Å, respectively. The maximum deviation from the best plane within the pyridine ring is −0.031(8) Å at C(2), and the dihedral angle between the two pyridine rings of a bpy is 3.0(2)°. The shortest Co(III)···Co(III) and Co(III)···Co(II) separations are 8.966(2) and 6.085(2) Å, respectively.

Magnetic Behavior of Compounds 1−3. The thermal dependence of the $\chi_M T$ product (χ_M is the magnetic susceptibility per two Co(II) ions) for compounds **1** and **3** is shown in Figure 4. The $\chi_M T$ versus T plot for **2** is very close to that of **1**, and it has been omitted for the sake of clarity. At room temperature, the values of $\chi_M T$ are 6.1 (**1** and **2**) and 7.2 (**3**) cm^3 mol^{-1} K. These values are as expected for two weak interacting high-spin Co(II) ions (**1**−**3**) and an isolated paramagnetic Ni(II) ion (**3**). The presence of this nickel(II) ion in **3** accounts for its greater values of $\chi_M T$ (the value of $\chi_M T$ for a triplet with $g = 2.0$ is ca. 1.0 cm^3 mol^{-1} K). Upon cooling, $\chi_M T$ decreases monotonically for **1**−**3** due to both antiferromagnetic interactions and spin−orbit coupling effects. At low temperatures, $\chi_M T$ attains a nearly constant value of ca. 1 cm^3 mol^{-1} K (**3**) and a minimum at ca. 10 K (**1** and **2**) under an applied low magnetic field ($H = 50$ G). Then, a maximum of $\chi_M T$ occurs at 6.5 (**1**) and 5.5 (**2**) K, and in the very low-temperature range, $\chi_M T$ varies linearly with T and it vanishes. These features are shown in the insert of Figure 4. The χ_M versus T plot for **1** and **2** exhibits a maximum about 12 K and a rapid increase for $T < 10$ K. No maximum of magnetic susceptibility is observed for **3**. A ferromagnetic phase transition related to a spin canting would account for the magnetic behavior of compounds **1** and **2**. Its occurrence was established by magnetization measurements (M) at low magnetic fields (H). When **1** and **2** are cooled in a low field (ca. 50 G), their magnetization (see Figure 5) exhibits a sharp transition below 9.0 (**1**) and 7.2 (**2**) K and then it approaches a saturation value of ca. 50 cm^3 mol^{-1} G (0.009 μ_B). This value is far away from that expected for two high-spin Co(II) ions indicating that a very small canting angle occurs. The critical temperature (T_c) is taken here as the maximum of

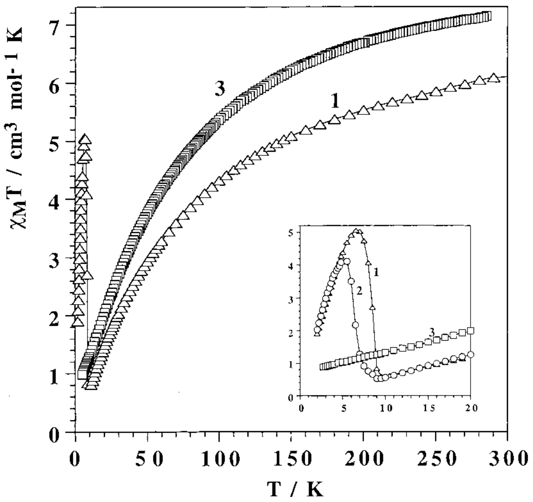

Figure 4. Thermal variation of $\chi_M T$ for compounds **1** (△) and **3** (□) at $H = 1000$ G. The inset shows the $\chi_M T$ behavior of compounds **1**−**3** at low temperatures and $H = 50$ G.

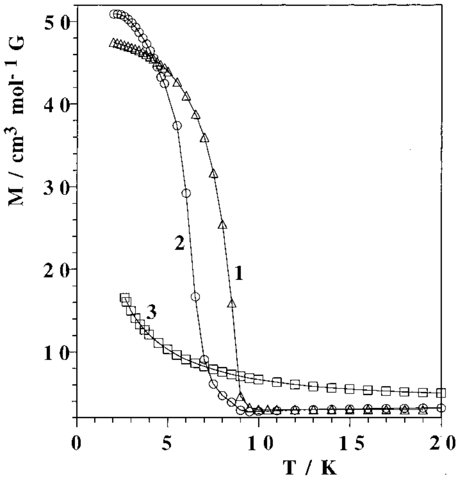

Figure 5. Plots of the field-cooled magnetization (M) for compounds **1** (△), **2** (○), and **3** (□) at $H = 50$ G.

---

(43) Hodgson, D. J.; Ibers, J. A. *Acta Crystallogr., Sect. B* **1969**, *25*, 469.

(44) Ohashi, Y.; Yanagi, K.; Mitsuhashi, Y.; Nagata, K.; Kaizu, Y.; Sasada, Y.; Kobayashi, H. *J. Am. Chem. Soc.* **1979**, *101*, 4739.

(45) Szalda, D. J.; Creutz, C.; Mahajan, D.; Sutin, N. *Inorg. Chem.* **1983**, *22*, 2372.

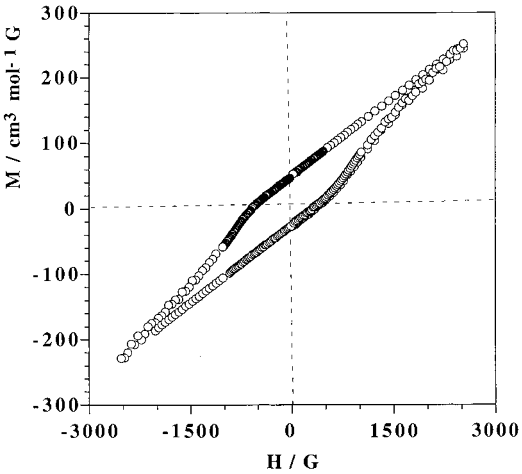

Figure 6. Magnetic hysteresis loop of compound **1** at 2 K.

the slope dM/dT: $T_c = 8$ (**1**) and 6 (**2**) K. Compound **3** exhibits paramagnetic behavior.

The magnetic hysteresis loop for **1** at 2 K is shown in Figure 6. The values of the coercive field (H_c) and remnant magnetization (M_r) are 500 G and 50 cm^3 mol^{-1} G, respectively. A similar hysteresis loop is observed for **2** with $H_c = 300$ G and $M_r = 40$ cm^3 mol^{-1} G.

It is well-known that the occurrence of spin canting can be due either to (i) antisymmetrical magnetic exchange or to (ii) magnetic anisotropy. The antisymmetrical magnetic exchange is precluded when an *n*-fold rotation axis is present at the bridging unit level. In our family of complexes a 2-fold axis occurs within the $(ox)_2Co^{II}(ox)Co^{II}(ox)_2$ unit and, consequently, the observed spin canting has to be attributed to the magnetic anisotropy. The magnetic anisotropy in our compounds is related to the well-known local anisotropy of octahedral high-spin Co^{II} and to the lack of inversion center in the crystal lattice. It is interesting to note that the structure of complexes **1**−**3** is chiral despite its cubic symmetry and, thus, the occurrence of an inversion center is precluded. In fact, similar structures with paramagnetic divalent metal ions having a smaller anisotropy, such as Mn^{II} or Fe^{II}, exhibit an antiferromagnetic ordering,[29] and consequently, no ferromagnetic ordering was observed.

We finish the present work with a brief comment on a very interesting point: given that the spin canting is associated with the chiral 3D $[Co_2(ox)_3]^{2-}$ network which is common to **1**−**3**, why is the value of T_c for **1** and **2** somewhat different and why is the spin canting structure lacking for **3**? It is clear that these features would be related to the different nature of the tris-chelated $[M(bpy)_3]^{n+}$ unit (M = Co(III), Fe(II), Ni(II). Its size follows the trend Co^{III} < Fe^{II} < Ni^{II} (average M−N bond length is 1.92, 1.98, and 2.09 Å, respectively; the values of the volume of the $[M(bpy)_3]^{n+}$ unit calculated through the expression $V = {}^4/_3\pi R^3$, R being either the Co(III)···C(3), Fe(II)···C(5), or Ni(II)···C(3) distance, are 431.6, 446.1, and 473.4 Å^3, respectively), and the smaller it is, the more favored the spin canting seems to be. To test these observations, further work using other tris-chelated $[ML_3]^{n+}$ species (M^{n+} and L being transition metal ions and bidentate type ligands, respectively) needs to be carried out.

Acknowledgment. Financial support from the Spanish Dirección General de Investigación Científica y Técnica (DGICYT) through Project PB94-1004 and from the European Community (TMR Programme) through Contract ERBFMRXCT980181 is gratefully acknowledged. Thanks are also extended to the Departamento de Química Inorgánica de la Universidad de La Laguna, La Laguna, Spain, for providing the chemical equipment and to Dr. F. V. Rodríguez-Romero for helpful discussions.

Supporting Information Available: Tables of crystal data, anisotropic displacement parameters for non-hydrogen atoms, atomic fractional coordinates, nonessential bond lengths and angles, and least-squares planes for **1** (8 pages). Ordering information is given on any current masthead page.

IC980306V